Astron. Astrophys. 334, L45–L48 (1998)

ASTRONOMY AND ASTROPHYSICS

LETTER

Letter to the Editor

HST observations of the QSO pair Q1026–0045A,B*

Patrick Petitjean[1,2], **Jean Surdej**[3,7], **Alain Smette**[4], **Peter Shaver**[5], **Jan Mücket**[6], **and Marc Remy**[3]

[1] Institut d'Astrophysique de Paris – CNRS, 98bis Boulevard Arago, F-75014 Paris, France
[2] UA CNRS 173-DAEC, Observatoire de Paris-Meudon, F-92195 Meudon Principal Cedex, France
[3] Institut d'Astrophysique, Université de Liège, Avenue de Cointe 5, B-4000 Liège, Belgium
[4] NASA-Goddard Space Flight Center, Code 681, Greenbelt, MD 20771, USA
[5] European Southern Observatory, Karl-Schwarzschild-Strasse 2, D-85748 Garching bei München, Germany
[6] Astrophysikalisches Institut Potsdam, An der Sternwarte 16, D-14482 Potsdam, Germany
[7] Directeur de Recherches du FNRS, Belgium

Received 12 February 1998 / Accepted 23 April 1998

Abstract. The spatial distribution of the Lyα forest is studied using new HST data for the quasar pair Q 1026–0045 A and B at $z_{\rm em}$ = 1.438 and 1.520 respectively. The angular separation is 36 arcsec and corresponds to transverse linear separations between lines of sight of $\sim$300h_{50}^{-1} kpc ($q_{\rm o}$ = 0.5) over the redshift range 0.833 $< z <$ 1.438. From the observed numbers of coincident and anti-coincident Lyα absorption lines, we conclude that, at this redshift, the Lyα structures have typical dimensions of $\sim$500h_{50}^{-1} kpc, larger than the mean separation of the two lines of sight. The velocity difference, ΔV, between coincident lines is surprisingly small (4 and 8 pairs with $\Delta V <$ 50 and 200 km s^{-1} respectively).

Metal line systems are present at $z_{\rm abs}$ = 1.2651 and 1.2969 in A, $z_{\rm abs}$ = 0.6320, 0.7090, 1.2651 and 1.4844 in B. In addition we tentatively identify a weak Mg II system at $z_{\rm abs}$ = 0.11 in B. It is remarkable that the $z_{\rm abs}$ = 1.2651 system is common to both lines of sight. The system at $z_{\rm abs}$ = 1.4844 has strong O VI absorption.

There is a metal-poor associated system at $z_{\rm abs}$ = 1.4420 along the line of sight to A with complex velocity profile. We detect a strong Lyα absorption along the line of sight to B redshifted by only 300 km s^{-1} relatively to the associated system. It is tempting to interpret this as the presence of a disk of radius larger than 300h_{50}^{-1} kpc surrounding quasar A.

Key words: quasars: individual: Q 1026–0045A,B, galaxies: ISM, quasars:absorption lines, galaxies: halo

1. Introduction

One way to probe the transverse extension of the gaseous structures giving rise to the Lyα forest seen in the spectrum of quasars is to observe multiple lines of sight to quasars with small angular separations on the sky and search the spectra for absorptions coincident in redshift.

This technique originated with a suggestion by Oort (1981) to test the possibility that the Lyα forest clouds originate in large pancake structures. The first discoveries of common and associated absorption using pairs of distinct quasars (with separations $\sim$ 1 arcmin) were made by Shaver et al. (1982) and Shaver & Robertson (1983). These already indicated the possible existence of very large absorber sizes (hundreds of kpc), even for the Lyα clouds. At about the same time Sargent et al. (1982) found no detectable tendency for Lyα lines to correlate in QSO pairs separated by a few arcmin. Spectra of pairs of gravitational lens images revealed common absorptions on smaller scales (Weyman & Foltz 1983, Foltz et al. 1984). The idea that Lyα clouds might have large sizes remained controversial untill the analysis by Smette et al. (1992), later confirmed by Dinshaw et al. (1994), Bechtold et al. (1994), Crotts et al. (1994), Bechtold & Yee (1994), Smette et al. (1995), D'Odorico et al. (1998).

Recently, Dinshaw et al. (1995) derived a radius of 330h_{50}^{-1} kpc at $z \sim$ 0.7 for spherical clouds from observation of Q0107–0232 and Q0107–0235 separated by 86 arcsec. Larger separations have been investigated by Crotts & Fang (1997) and Williger et al. (1997). Both studies conclude that the clouds should be correlated on scales larger than 500 kpc.

Here we present observations of Q1026–005 A ($m_{\rm r}$ = 18.4, $z_{\rm em}$ = 1.438) and B ($m_{\rm r}$ = 18.5, $z_{\rm em}$ = 1.520), two distinct quasars separated on the sky by 36 arcsec or 300 h_{50}^{-1} kpc ($q_{\rm o}$ = 0.5) at $z \sim$ 1.

2. Observations

The observations were carried out on the Hubble Space Telescope using the Faint Object Spectrograph with the G270H grating over the wavelength range 2250–3250 Å, for a resolution of 1.92 Å FWHM. A total of 5300 s integration time was accumulated on both quasars. The data were calibrated using the

Send offprint requests to: Patrick Petitjean (petitjean@iap.fr)

* Based on observations obtained with the NASA/ESA *Hubble Space Telescope* by the Space Telescope Science Institute, which is operated by AURA, Inc., under NASA contract NAS 5-26555

standard pipeline reduction techniques. The zero point of the wavelength scale was determined requiring that Galactic interstellar absorptions occur at rest. Most of the lines are weak or blended except Mg IIλ2803; the error on the wavelength determination should be smaller than 0.3 Å however. The spectra are shown in Fig. 1, the line–lists are given in Table 1. The position of absorption features are determined by gaussian fits. Lower limits on equivalent widths of Lyα lines are at the 3σ level. The mean signal to noise ratio is 15 varying from 10 in the very blue to 20 on top of the Lyα emission lines.

3. Results

3.1. The metal line systems

Metal line systems are present at $z_{\rm abs}$ = 1.2651 and 1.2969 in A, $z_{\rm abs}$ = 0.11, 0.6320, 0.7090, 1.2651 and 1.4844 in B.

In A, the system at $z_{\rm abs}$ = 1.2651 is detected by strong H I$\lambda\lambda$1025,1215 absorptions and has a Si IV$\lambda\lambda$1393,1402 doublet associated. There are strong H I$\lambda\lambda$1025,1215 absorptions at the same redshift along the line of sight to B. The fact that the positions of the H I absorptions in A and B are nearly identical (λ2753.67 and λ2753.74 Å for Lyα respectively) argues for the two absorptions being produced by the same object. If true the transverse dimension is larger than the 310 h_{50}^{-1}kpc separation between the two lines of sight. The system at $z_{\rm abs}$ = 1.2969 has strong H I ($w_{\rm r}$(Lyα) = 2.9 Å), C II, C III, O I, N III, Si II, Si III, Si IV absorptions.

In B, both $z_{\rm abs}$ = 0.6320 and 0.7090 systems have strong Si IIλ1526, Fe IIλ1608, Al IIλ1670 and C IVλ1550 absorptions. As said before the $z_{\rm abs}$ = 1.2651 system is common to A and B. The presence of metals is revealed only by a λ3155.87 feature that we identify as Si IVλ1393. The associated Si IVλ 1402 line is not detected but could be lost in the noise. The strong system at $z_{\rm abs}$ = 1.4842 shows N III, C III, Si III and possibly O VI associated absorptions. O VI absorption seems to be detected in most of the low and intermediate redshift systems (Bergeron et al. 1994, Vogel & Reimers 1995, Burles & Tytler 1996) and has been observed in a few high redshift Lyman limit systems (Kirkman & Tytler 1997). Although the velocity difference with the quasar is larger than 4000 km s^{-1}, there is a possiblility that the system is associated with the quasar. In addition we tentatively identify a weak ($w_{\rm r}\sim$ 0.3Å) Mg II system at $z_{\rm abs}$ = 0.11 in B. Mg IIλ2803 is possibly blended with C IVλ1548 of a possible weak C IV system at $z_{\rm abs}$ = 1.0106.

3.2. The associated system in A and the proximity effect

There is a strong associated system detected in A by its H I Lyα and Lyβ absorptions. Two components are seen at $z_{\rm abs}$ = 1.4401 and 1.4420 with $w_{\rm r}$(Lyα) = 0.58 and 0.40 Å respectively. The two components are *redshifted* relative to the QSO by 260 and 490 km s^{-1}. Since the true redshift of the quasar is poorly known, these values are very uncertain. We do not detect any metal lines in the system. The O VI lines have $w_{\rm r}$ < 0.20 Å; the C IV lines are redshifted outside the wavelength range of the data. Interestingly enough, there is a H I absorption system

Table 1. Line list

	Q1026-0045A $\lambda_{\rm obs}$ (Å)	$w_{\rm obs}$ (Å)	Ident.	z		Q1026-0045B $\lambda_{\rm obs}$ (Å)	$w_{\rm obs}$ (Å)	Ident.	z	(a)
					1	2229.2:	0.6:	SiII1304	0.7090	
1	2233.76	1.53	Lyγ	1.2968						
2	2244.20	1.10	CIII977	1.2970						
3	2259.87	0.51	Lyα	0.8589			<0.45			u/u/u
4	2273.23	0.55	NIII989	1.2967						
		<0.60			2	2274.68	0.67	SiIV1393	0.6320	
					3	2281.17	2.19	CII1334	0.7093	
		<0.65			4	2288.50	0.9:	Lyα	0.8825	u/u/u
								SiIV1402	0.6320	
					5	2312.30	0.49	Ly6	1.4843	
5	2319.2:	0.35	Lyδ	1.4419						
6	2323.54	1.28	Lyβ	1.2653	6	2323.65	0.73	Lyβ	1.2654	
		<0.40			7	2330.03	1.22	Lyα	0.9166	u/u/u
								Lyϵ 1.4846		
7	2338.16	1.32	Lyβ	1.2802	8	2337.93	0.50	Lyα	0.9231	u/u/u
					9	2344.34	0.50	FeII2344	0.0000	
8	2355.48	1.95	Lyβ	1.2964						
					10	2359.85	0.96	Lyδ	1.4847	
9	2368.92	1.28	Lyα	0.9486	11	2368.97	1.19	Lyα	0.9486	C/C/C
10	2375.03	2.08	Lyγ	1.4405	12	2376.05	1.51	Lyγ	1.4438	
			Lyγ	1.4419				FeII2344	0.0000	
			Lyα	0.9536				Lyα	0.9545	u/u/u
11	2380.26	0.77	CII1036	1.2968						
12	2382.97	0.90	FeII2382	0.0000	13	2382.25	1.52	FeII2382	0.0000	
								SiIV1393	0.7092	
13	2392.90	1.13	Lyα	0.9683			<0.38			u/A/u
					14	2397.06	0.56	SiIV1402	0.7088	
					15	2415.90	1.00	Lyγ	1.4841	
		<0.45			16	2419.8:	0.32	Lyα	0.9904	u/u/u
		<0.45			17	2424.53	0.42	Lyα	0.9943	u/u/u
					18	2427.30	0.65	CIII977	1.4844	
		<0.45			19	2444.15	0.85	Lyα	1.0105	u/A/u
14	2450.0:	0.75	Lyα	1.0153			<0.28			u/u/u
15	2454.0:	0.34	Lyα	1.0186	20	2454.32	0.63	Lyα	1.0189	A/A/u
16	2458.47	0.61	Lyα	1.0223	21	2458.65	0.30	NIII989	1.4840	A/A/u
17	2474.3:	0.25	Lyα	1.0353	22	2475.8	0.35	Lyα	1.0365	u/u/u
					23	2491.71	0.83	SiII1526	0.6321	
18	2497.51	1.29	Lyα	1.0544	24	2497.24	0.49	Lyα	1.0542	C/A/A
19	2503.30	1.30	Lyβ	1.4405						
20	2504.66	1.20	Lyβ	1.4419	25	2506.65	0.59	Lyβ	1.4438	
					26	2521.88	0.26	Lyα:	1.0744	u/u/u
		<0.38			27	2526.44	1.52	Lyα	1.0782	A/u/u
								CIV1548	0.6321	
					28	2531.03	0.46	CIV1550	0.6321	
					29	2548.25	1.22	Lyβ	1.4844	
					30	2563.70	0.84	OVI1031	1.4844	
21	2568.5:	0.38	Lyα	1.1128			<0.28			u/u/u
22	2575.22	1.70	Lyα	1.1183	31	2575.37	0.82	Lyα	1.1184	C/C/A
					32	2577.5:	0.59	OVI1037	1.4841	
23	2586.35	0.50	FeII2586	0.0000	33	2587.9:	0.42	FeII2586	0.0000	
24	2600.58	1.40	FeII2600	0.0000	34	2601.2:	1.23	FeII2600	0.0000	
					35	2608.74	0.79	SiII1526	0.7087	
					36	2625.28	0.51	FeII1608	0.6322	
					37	2645.44	0.83	CIV1548	0.7087	
					38	2650.08	0.67	CIV1550	0.7089	
		<0.35			39	2669.58	0.42	Lyα	1.1959	u/u/u
					40	2726.96	0.90	AlII1670	0.6321	
25	2733.15	1.06	SiII1190	1.2968						
			SiIII1206	1.2650						
26	2736.63	0.52	Lyα	1.2511			<0.25			A/u/u
27	2740.75	0.87	SiII1193	1.2968						
		<0.32			41	2745.29	0.75	Lyα	1.2582	A/A/u
					42	2748.47	0.63	FeII1608	0.7088	
28	2753.67	2.42	Lyα	1.2651	43	2753.74	1.50	Lyα	1.2651	M_c
29	2772.06	3.10	SiIII1206	1.2976						
			Lyα	1.2802						A/A/A
30	2792.35	6.62	Lyα	1.2969			<0.36			M_a
31	2796.05	2.20	MgII2796	0.0000	44	2796.90:	1.95	MgII2796	0.0000	
32	2803.60	1.17	MgII2803	0.0000	45	2803.54	0.98	MgII2803	0.0000	
33	2807.94	0.44	Lyα	1.3097			<0.36			u/u/u
34	2820.08	0.73	Lyα	1.3197	46	2819.87	0.74	Lyα	1.3195	C/C/u
35	2849.12	0.80	Lyα	1.3436			<0.24			A/A/u
					47	2854.78	1.10	AlII1670	0.7086	
36	2895.00	1.85	SiII1260	1.2969						
37	2961.76	0.28	Lyα	1.4363						
38	2966.45	0.97	Lyα	1.4401						
39	2968.69	1.42	Lyα	1.4420	48	2971.09	1.30	Lyα	1.4439	
40	2991.08	0.30	OI1302	1.2970						
41	2995.36	0.66	SiII1304	1.2964						
					49	2997.47	0.66	SiIII1206	1.4844	
					50	3008.06	0.40	Lyα	1.4743	
								AlIII1854:	0.6219	
					51	3020.05	1.75	Lyα	1.4842	
					52	3027.51:	0.53	AlIII1862:	0.6252	
42	3065.05	0.86	CII1334	1.2967						
					53	3104.81	0.36	MgII2796	0.1103	
					54	3113.13	0.30	MgII2803	0.1104	
								CIV1548?	1.0106	
					55	3118.00	0.20:	CIV1550?	1.0106	
43	3156.92	0.32	SiIV1393	1.2650	56	3155.87	0.57	SiIV1393?	1.2643	
					57	3168.43	0.44	AlIII1854?	0.7083	
44	3177.14	0.24	SiIV1402	1.2649						
45	3201.42	0.62	SiIV1393	1.2970						
46	3222.51	0.54	SiIV1402	1.2972						

(a) Coincidences are marked by a "C", anti-coincidences by a "A" and ambiguous cases by a "u" for $w_{\rm r}$ > 0.2, 0.3 and 0.6 Å.
* A colon means uncertain value or identification

at $z_{\rm abs}$ = 1.4439 along the line of sight to Q 1026–0045B. The velocity difference between this system and the $z_{\rm abs}$ = 1.4420 in A is about 230 km s^{-1} only.

It is unlikely that the $z_{\rm abs} \sim z_{\rm em}$ system is intrinsically associated with the central AGN. Such systems usually have high metal content and are expected to exhibit strong O VI and N V absorptions (Petitjean et al. 1994, Hamann 1997), absent from the spectra of Q1026–0045 A & B. The three absorptions are thus part of an object or group of objects which transversal dimension exceeds the $300h_{50}^{-1}$ kpc separation between the two lines of sight.

The absence of metals in the system associated with A, over the observed wavelength range, suggests an intergalactic origin. The higher velocity of the gas along the line of sight to B argues against the simple picture in which the gas would be collapsing toward A. In that case, we would expect the gas along the line of sight to B to have a projected velocity smaller than the velocity of the gas just in front of A. A model where the gas would be part of a rotating disk can be accomodated if the component at z = 1.4420 is at the same redshift as the quasar. In this case however one could wonder why the gas is metal deficient.

The relative equivalent widths of the hydrogen lines in the Lyman series of the system at $z_{\rm abs}$ = 1.4842 toward B are indicative of H I column densities in excess of 10^{16} cm^{-2}. The presence of strong metal lines suggests that the gas is associated with the halo of a galaxy. Very deep imaging in this field to search for any enhanced density of objects would help to understand the nature of these intriguing systems.

There are only two systems in both lines of sight from z = 1.3436 to 1.520, the associated system in A (and its counterpart in B) and the metal system at z = 1.4842 in B. The number of lines with $w_{\rm r} > 0.24$ Å expected in this redshift range is 7±2 (Bahcall et al. 1996). It is probable that we see the effect of the enhanced photo-ionizing field due to the proximity of the quasars.

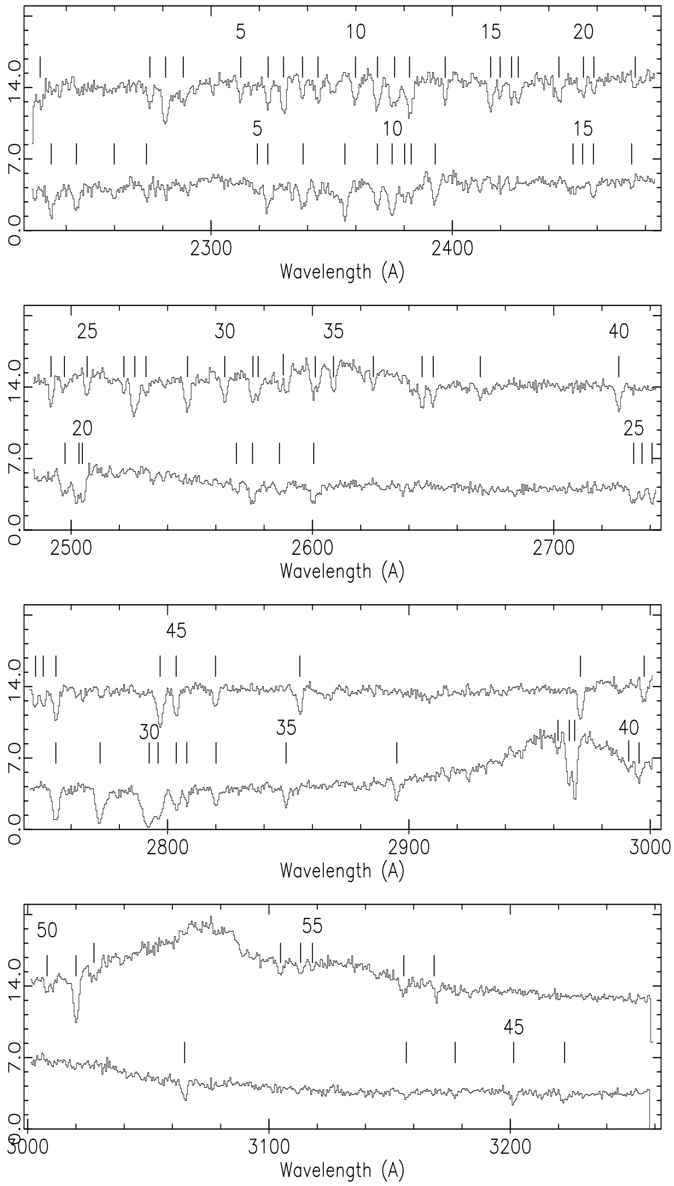

Fig. 1. Spectra of Q1026–0045 A (bottom) and B (top). Flux is given in units of 10^{-16} erg/s/cm^{-2}/Å. The spectrum of B has been shifted by 8.5 in the same units. Line identification can be found in Table 1.

3.3. *The Lyα forest*

3.3.1. The line-lists

Table 1 lists all the absorption features detected at the 3σ level in the spectra. Identification of Lyα lines is sometimes uncertain due to blending with lines from the numerous metal line systems. We discuss here individual lines.

In Q 1026–0045A, the λ2259 feature could be partly Lyϵ from the $z_{\rm abs}$ = 1.4420 system but given the strength of the other lines in the series, the contribution is most certainly negligible. There is a broad feature centered at 2452 Å that we decompose into two components at 2450 and 2454 Å. This feature is uncertain however. Galactic Fe IIλ2374 absorption should not contribute too much to the λ2375 feature that is mostly Lyγ at $z_{\rm abs}$ = 1.4405 and 1.4420. The line is quite strong however and could be partly produced by a Lyα absorption at $z_{\rm abs}$ = 0.9536. The two lines at λ2458 and λ2474 could correspond to a Si IVλ λ1393,1402 doublet at $z_{\rm abs}$ = 0.7639. The corresponding C IIλ 1334 line would be blended with Lyβ at $z_{\rm abs}$ = 1.2964 but the feature at λ2736 could be C IVλ1550 at the same redshift with no C IVλ1548 detected. The line however is displaced by more than 1 Å from the expected position which is not acceptable. We thus consider the Si IV identification as doubtful.

In Q 1026–0045B, there is a broad feature at λ2288.5 that cannot be accounted for by Si IVλ1402 at z = 0.6320 only. The feature at λ2376 may have a double structure. Lyγ at 1.4438 and Fe IIλ2374 definitively contribute to this feature which is strong enough however to be partly produced by Lyα absorption at $z_{\rm abs}$ = 0.9545. Since C IVλ1550 at $z_{\rm abs}$ = 0.6321 has $w_{\rm obs}$ = 0.46 Å, C IVλ1548 at the same redshift should have $w_{\rm obs} < 0.92$ Å. Consequently there is a Lyα line at $z_{\rm abs}$ = 1.0782 with $w_{\rm obs} > 0.6$ Å.

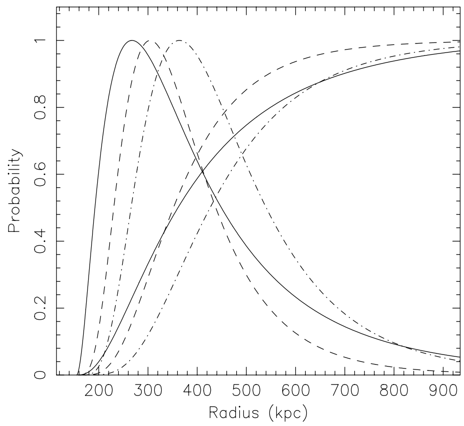

Fig. 2. Probability distribution $P(R)$, normalized to one at its peak, and cumulative distribution versus cloud radius from the number of coincidences and anticoincidences of Lyα lines with $w_\mathrm{r} > 0.2$ (dashed-dotted lines), 0.3 (dashed lines) and 0.6 Å(solid lines). The peak of the probability is at R = 267, 305 and $364h_{50}^{-1}$ kpc for $w_\mathrm{r} > 0.6$, 0.3 and 0.2 Å respectively.

We detect 11 and 12 Lyα lines with $w_\mathrm{r} > 0.2$ Å over the redshift range 0.8335–1.3436 along the lines of sight to A and B respectively. The density of lines with $w_\mathrm{r} > 0.24$ Å detected by the HST in the same redshift range is $\sim$17$\pm$3 (Jannuzi et al. 1998). The number of lines we detect is thus small. This might be a consequence of blending effects. Two lines observed along A and B are said coincident when their redshifts are within 200 km s^{-1}. The Lymanα forest is sparse at low redshift which implies that the probability for random coincidence is negligible (only 0.05 for $w_\mathrm{r} > 0.2$ Å). Last column of Table 1 indicates for each Lyα line with $w_\mathrm{r} > 0.2$, 0.3, 0.6 Å whether there is coincidence (C) or anti-coincidence (A). A letter (u) marks lines that are out of the sample or uncertain cases because of blending effets.

3.3.2. Correlations

The numbers of coincidences and anticoincidences for $w_\mathrm{r} > 0.2$, 0.3 and 0.6 Å are 4, 3, 1 and 7, 8, 3 respectively. Assuming that the Lyα clouds are spheres of radius R, we calculate the probability density for R (see Fig. 2) following Fang et al. (1996). The peak of the probability is at R = 267, 305 and $364h_{50}^{-1}$ kpc for $w_\mathrm{r} > 0.6$, 0.3 and 0.2 Å. There is a hint for the dimensions of the structures to be larger for smaller equivalent widths. This property is expected in simulations (Charlton et al. 1997). However as shown by Fang et al. (1996) and Crotts & Fang (1997), the radius determined by this method increases with the separation of the lines of sight indicating that the assumption of a single structure size is invalid. This has been recognized to be a characteristic of the spatial distribution of the Lyα gas in the simulations (Charlton et al. 1997). It is clear that better statistics in the data are needed to have a better understanding of the structures especially to discuss the difference between real size of the clouds and correlation length (Cen & Simcoe 1997).

It is intriguing to note that the velocity difference ΔV between lines coincident in redshift along the two lines of sight is small. Considering all the pairs, we find 4 and 8 pairs with $\Delta V < 50$ and 200 km s^{-1} respectively. There is no pair, even along one single line of sight with $200 < \Delta V < 400$ km s^{-1}. This has been shown to favor disk-like structures (Charlton et al. 1995) but should be studied in more detail.

Acknowledgements. MR and JS wish to thank the SSTC/PRODEX project for partial support during this work.

References

Bahcall J.N., Bergeron J., Boksenberg A., et al., 1996, ApJ 457, 19

Bechtold J., Crotts A.P.S., Duncan R.C., Fang Y., 1994, ApJ 437, L83

Bechtold J., Yee H.K.C., 1994, AJ 110, 1984

Bergeron J., Petitjean P., Sargent W.L.W., et al., 1994, ApJ 436, 33

Burles S., Tytler D., 1996, ApJ 460, 584

Cen R., Simcoe R.A., 1997, ApJ 483, 8

Charlton J.C., Anninos P., Zhang Y., Norman M.L., 1997, ApJ 485, 26

Charlton J.C., Churchill C.W., Linder S.M., 1995, ApJ 452, L81

Crotts A.P.S., Bechtold J., Fang Y., Duncan C., 1994, ApJ 437, 79

Crotts A.P.S., Fang Y., 1997, astro-ph 9702185

Dinshaw N., Foltz C.B., Impey C.D., Weymann R.J., Morris S.L., 1995, Nature 373, 223

Dinshaw N., Impey C.D., Foltz C.B., Weymann R.J., Chaffee F.H.Jr., 1994, ApJ 437, L87

D'Odorico S., Cristiani S., D'Odorico V., et al., 1998, in P. Petitjean & S. Charlot, XIII^e IAP Colloquium, Editions Frontières, Paris, p. 392

Fang Y., Duncan R.C., Crotts A.P.S., Bechtold J., 1996, ApJ 462, 77

Foltz C.B., Weymann R.J., Röser H.J., Chaffee F.H.Jr., 1984, ApJ 281, L1

Hamann F., 1997, ApJS 109, 279

Jannuzi B., et al., 1998, ApJS in press

Kirkman D., Tytler D., 1997, ApJ 489, L123

Oort J.H., 1981, A&A, 94, 359

Petitjean P., Rauch M., Carswell R.F., 1994, A&A 291, 29

Sargent L.W.L., Young P., Schneider D.P., 1982, ApJ 256, 374

Shaver P.A., Boksenberg A., Robertson J.G., 1982, ApJ 261, L7

Shaver P.A., Robertson J.G., 1983, ApJ 268, L57

Smette A., Robertson J.G., Shaver P.A., et al., 1995, A&AS 113, 199

Smette A., Surdej J., Shaver P.A., et al., 1992, A&A 389, 39

Vogel S., Reimers D., 1995, A&A 294, 377

Weymann R.J., Foltz C.B., 1983, ApJ 272, L1

Williger G.M., Smette A., Hazard C., Baldwin J.A., McMahon R.G., 1997, astro-ph/9709170